Med Chem Res (2011) 20:421–429
DOI 10.1007/s00044-010-9330-5

MEDICINAL CHEMISTRY RESEARCH

ORIGINAL RESEARCH

Synthesis, characterization, antibiogram and DNA binding studies of novel Co(II), Ni(II), Cu(II), and Zn(II) complexes of Schiff base ligands with quinoline core

Gurunath S. Kurdekar · Sathisha Mudigoudar Puttanagouda · Naveen V. Kulkarni · Srinivasa Budagumpi · Vidyanand K. Revankar

Received: 13 August 2009 / Accepted: 16 February 2010 / Published online: 12 March 2010

Abstract A series of Co(II), Ni(II), Cu(II), and Zn(II) complexes of Schiff base ligands L^1H_3 and L^2H have been prepared. The ligands are synthesized by the condensation of 2-hydroxy-3-formylquinoline with salicyloylhydrazide and 2-hydrazinobenzothiazole in absolute ethanol. The prepared complexes were characterized by the analytical and spectral techniques. The stoichiometry of the complexes is found to be 1:1. The presence of coordinated and lattice water is confirmed by the TG and DTA studies. Subsequently all the prepared complexes were screened for antimicrobial activity against bacteria and fungi. The Cu(II) complexes have been found to be more active than the ligand. In addition the DNA binding/cleaving capacity of the compounds was analyzed by absorption spectroscopy, viscosity measurement, thermal denaturation, and gel electrophoresis methods.

Keywords Quinoline · Salicyloylhydrazide · 2-Hydrazinobenzothiazole · Antimicrobial activity DNA binding study

Introduction

Schiff base ligands have been studied extensively for years, due to the synthetic flexibilities, selectivity as well as sensitivity toward the transition metal ions. The architectural beauty of these coordination complexes arises due to the interesting ligand systems containing different donor sites in heterocyclic rings. Among the ligand systems, quinoline derivatives of hydrazone occupy special place because, these ligands developed due to their diverse chelating capability, structural flexibility (Rao *et al*., 1997) and pharmacological activities like antibacterial, antifungal, antitumoural, antiviral, antimalarial, antituberculosis (West *et al*., 1993). In addition to this, the interaction of these Schiff base metal complexes with DNA has been extensively studied in the past decades. Due to the site-specific binding properties and many fold applications in cancer therapy, these coordination compounds were suitable candidates as DNA secondary structure probes, photo cleavers, and antitumor drugs (Chan and Wong, 1995; Pratviel *et al*., 1998; Liang *et al*., 2004). The design of small complexes that bind/react at site-specific sequences of DNA becomes important as they can draw significant structural perturbations in the host. DNA is an important cellular receptor, many chemicals exert their antitumor effects through binding to DNA thereby changing the replication of DNA and inhibiting the growth of the tumor cells. This is the fundamental facet of designing new and more efficient antitumor drugs and their effectiveness depends on the mode and affinity of the binding. A more complete understanding of how to target DNA sites with specificity will lead not only to novel chemotherapeutics but also to a greatly expanding ability for chemists to probe DNA and to develop highly sensitive diagnostic agents (Erkkila *et al*., 1999).

The coordination of quinoline has gained increasing attention as antibacterials (Freixas and Span, 1991; Ryoichi *et al*., 1991), monoamine oxidase inhibitors (Gracheva *et al*., 1988), and herbicides (Hagen *et al*., 1988). On the other hand, substituted quinolines are prominent building blocks in both organic and inorganic molecular chemistry with their π-stacking ability and coordination properties.

G. S. Kurdekar · S. Mudigoudar Puttanagouda · N. V. Kulkarni · S. Budagumpi · V. K. Revankar (✉)
Department of Chemistry, Karnatak University, Pavate Nagar, Dharwad 580 003, Karnataka, India
e-mail: vkrevankar@rediffmail.com

Specially, the 3-substituted 2-hydroxyquinolines show tautomeric forms at 2- position of the heterocycle and easily form a lactum tautomer. The interesting thing in the study of these compounds is the existence of lactum tautomer in presence of a transition metal ion. Furthermore, the ligands designed in the present investigation, in such a way, the complexes derives are associated at least with one labile chloride to interact with the N-7 of nucleotide after deprotonation. These observations prompted us to prepare a series of quinoline Schiff base later first row transition metal (II) complexes with the 3-substituted 2-hydroxyquinoline derivatives.

Experimental

Chemistry

Materials and methods

All the chemicals used were of reagent grade and the solvents were distilled before use according to the standard procedure. The preparation of 2-hydroxy-3-formylquinoline (Meth-Cohn and Narine, 1978), salicyloylhydrazide (Vogel, 1968), and 2-hydrazinobenzothiazole (Revankar *et al*., 1990) were prepared according to the reported methods. The metal salts used were in the hydrated form.

Preparation of the Schiff base ligands

A hot ethanolic solution of 2-hydroxy-3-formylquinoline (0.005 mol, 25 ml), salicyloylhydrazide (0.005 mol, 25 ml) was added in ethanolic solution, which was refluxed for about 3-4 h on a water bath. The resulting solid product was filtered in hot condition [yield- 80%].

The same procedure was followed for the preparation of the ligand L^2H by using 2-hydrazinobenzothiazole, [yield-70%] (The structure of both the ligands shown in Fig. 1).

Preparation of complexes

To the hot solution of ligand in ethanol (0.004 mol in 25 ml), an ethanolic solution of the metal chloride (0.004 mol in 25 ml) was added drop wise and stirred for an hour. The mixture was heated to reflux for 3–5 h to get complex in solid form. The product was filtered off, washed several times with ethanol, and dried in vacuum over P_2O_5.

Biochemistry

Anti-biogram analysis against bacteria and fungi is done as per the well reported method (Seeley 1991).

The samples showing significant inhibition were selected for the further determination of (Minimum Inhibitory Concentrations) MICs.

DNA binding studies

Isolation of DNA DNA was isolated using the procedure mentioned below:

The fresh bacterial culture (1.5 ml) was centrifuged to obtain the pellet. So obtained pellet was dissolved in 0.5 ml of lysis buffer (100 mM tris pH 8.0, 50 mM EDTA, 50 mM lysozyme) and 0.5 ml of saturated phenol was added to it and incubated at 55°C for 10 min, and then centrifuged at 10,000 rpm for 10 min. To the supernatant liquid equal volume of chloroform: isoamyl alcohol (24:1) mixture and 1/20th volume of 3 M sodium acetate (pH 4.8) was added. Again it was centrifuged at 10,000 rpm for 10 min and to the supernatant 3 volumes of chilled absolute alcohol added. The precipitated DNA was separated by centrifugation. The pellet was dried and dissolved in TE buffer (10 mM tris pH 8.0, 1 mM EDTA) and stored in cool place.

Concentration measurement The concentration of *E. coli* DNA per nucleotide [C(p)] was measured by using its known extinction coefficient at 260 nm (6600 M–1 cm^{-1}) (Sarma, 1980). The absorbance at 260 nm (A260) and at 280 nm (A280) for *E. coli* was measured to check its purity. The ratio A260/A280 was found to be 1.84, indicating that *E. coli* was satisfactorily free from protein. Buffer [5 mM tris(hydroxymethyl) amino methane, tris, pH 7.2, 50 mM NaCl] was used for the absorption, viscosity, and thermal denaturation experiments.

Absorption studies

In absorption studies the complex was dissolved in DMSO and then diluted to the desired concentration with water.

Fig. 1 Structure of the ligands

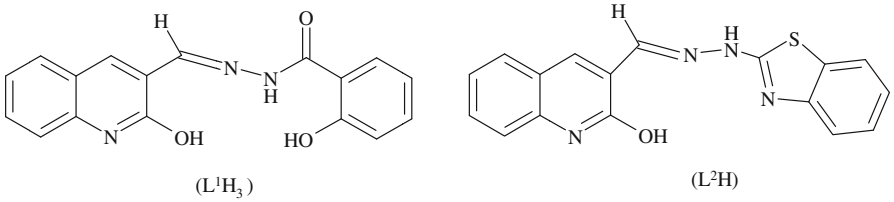

(L^1H_3) (L^2H)

The spectroscopic titrations were carried out by adding increasing amounts of *E. coli* DNA to a solution of the complex at a fixed concentration contained in a quartz cell, UV-Vis spectra were recorded after equilibration at 23°C for 10 min after each addition. The intrinsic binding constant Kb was determined from the plot of $A_0/[A - A_0]$ vs. $[\text{DNA}]^{-1}$ according to equation (Dang *et al*., 1998).

$$A_0/[A - A_0] = \varepsilon_G/[\varepsilon_{H-G} - \varepsilon_G] + \varepsilon_G/[\varepsilon_{H-G} - \varepsilon_G] \times 1/K[\text{DNA}] \quad (1)$$

where A_0 and A are the absorbance observed for MLCT absorption band for the free complex and absorbance observed for MLCT absorption band at given DNA concentration, respectively. [DNA] is the concentration of DNA in base pairs, ε_G and ε_{H-G} are the apparent absorption coefficients in free and DNA bounded form of complex, respectively. The data were fitted into the above equation to obtain a graph, with a slope equal to $\varepsilon_G/[\varepsilon_{H-G} - \varepsilon_G] \times 1/K$ and intercept equal to $\varepsilon_G/[\varepsilon_{H-G} - \varepsilon_G]$ hence Kb was obtained from the ratio of the intercept to the slope.

Viscosity measurements

Viscosity measurements were carried out using an Ostwald micro-viscometer, maintained at constant temperature (23°C) in a thermostat bath. The DNA concentration was kept constant in all samples, but the complex concentration was increased each time (from 20 to 80 μM). Mixing of the solution was achieved by bubbling the nitrogen gas through viscometer. The flow time was measured with a digital stopwatch. The sample flow times were measured three times and the mean value was used. Data are presented as $(\eta/\eta_0)^{1/3}$ versus the ratio [complex]/[DNA], where η and η_0 are the specific viscosity of DNA in presence and in absence of the complex, respectively. The values of η and η_0 were calculated by using Eq. 2,

$$\eta = (t - t^b)/t^b \quad (2)$$

where t is the observed flow time of DNA containing solution upon the addition of compounds and t^b is the flow time of DNA containing solution alone. Relative viscosities for DNA solution were calculated from the relation (η/η_0) (Satyanarayana *et al*., 1992).

Thermal denaturation studies

These were carried out on UV-spectrometer, equipped with temperature controlling thermostat. The melting curves (T_m) of both free *E. coli* DNA and *E. coli* DNA bound complexes were obtained by measuring the hyperchromicity of *E. coli* DNA at 260 nm as a function of temperature. The melting temperatures were measured with 45 μM DNA in phosphate buffer at pH 6.8 ($\mu = 0.2$ M NaCl). The temperature was scanned from 25 to 80°C at a speed of 5°C per min. The melting temperature (T_m) was taken as the mid-point of the hyperchromic transition.

DNA cleavage experiment

Culture media: Potato dextrose broth (Peptone 10, NaCl 10 and yeast extract 5 g/l) was used for the growth of the *E. coli*. The 50 ml media was prepared, autoclaved for 15 min at 121°C and 15 lb pressure. The autoclaved media was inoculated with the seed culture and incubated at 37°C for 24 h.

Treatment of DNA with the samples: The samples (10 mg/ml) were prepared in DMSO. The synthesized compounds (100 μg) were added separately to the DNA sample of *E. coli*. The samples mixtures were incubated at 37°C for 2 h.

Agarose gel electrophoresis

The 200 mg of agarose was weighed and dissolved it in 25 ml of TAE buffer (4.84 g Tris base, pH 8.0, 0.5 M EDTA/l) by boiling. When the gel attained the temperature of ~55°C, it was poured into the gel cassette fitted with comb. Then the comb was removed carefully and the solidified gel was placed in the electrophoresis chamber flooded with TAE buffer. To this electrophoresis chamber 20 μl of DNA sample (mixed with bromophenol blue dye at 1:1 ratio) was loaded carefully into the wells, along with standard DNA marker and the constant 50 V of electricity was supplied to it for around 30 min. After 30 min the gel was removed carefully and stained with Ethidium Bromide (ETBR) solution (10 μg/ml) and the bands were observed under UV trans-illuminator for 10–15 min.

Analysis and physical measurement

The metal estimation was done by standard methods. Carbon, hydrogen, and nitrogen analysis were carried out on a Thermo quest elemental analyser. The molar conductance measurements were made on an ELICO-CM-82 conductivity bridge with a cell having cell constant of 0.51 cm^{-1}. The magnetic measurements were made with Faraday Balance at room temperature by using $Hg[Co(SCN)_6]$ as calibrant. The electronic spectra of compounds in DMSO were recorded using VARIAN CARY 50 Bio UV-visible spectrophotometer. The IR spectra of ligands and their complexes were recorded as KBr pellets in the region 4000–400 cm^{-1} on Nicolet 170 SX FT-IR spectrometer. The ^1H NMR spectra of ligands and zinc(II) complexes were recorded in DMSO-d_6 on Bruker 300 MHz spectrometer using TMS as an internal standard. The EPR spectra of copper(II) complexes were

Table 1 Analytical, conductivity, and magnetic data for the ligands and their complexes

Compounds abbreviations	Compounds	Found (Calculated)						Conductivity	Magnetic moment μ_{eff} BM
		C	H	N	S	M	Cl		
L^1H_3	$C_{17}H_{13}O_3N_3$	65.7 (66.4)	4.0 (4.2)	13.1 (13.6)	–	–	–	–	–
C1	[Co $L^1Cl{\cdot}2H_2O]{\cdot}H_2O$	44.2 (44.9)	3.4 (3.9)	8.9 (9.2)	–	12.6 (12.9)	7.4 (7.8)	15	4.43
C2	[Ni $L^1Cl{\cdot}2H_2O]{\cdot}H_2O$	44.5 (44.9)	3.3 (3.9)	9.0 (9.2)	–	12.4 (12.9)	7.4 (7.8)	18.4	2.95
C3	[Cu $L^1Cl]_2{\cdot}4H_2O$	46.1 (46.3)	2.3 (2.7)	9.4 (9.5)	–	14.1 (14.4)	7.7 (7.9)	22.3	1.69
C4	[Zn $L^1Cl{\cdot}2H_2O]{\cdot}H_2O$	43.7 (44.1)	3.5 (3.8)	8.6 (9.0)	–	13.7 (14.1)	7.2 (7.6)	12.1	Diamagnetic
L^2H	$C_{17}H_{12}ON_4S$	63.3 (63.7)	3.4 (3.7)	17.2 (17.5)	9.6 (10)	–	–	–	–
C5	[Co $L^2Cl{\cdot}2H_2O$]	45.1 (45.4)	2.9 (3.3)	12.1 (12.4)	6.8 (7.1)	12.8 (13.1)	6.5 (7.9)	17.5	4.45
C6	[Ni $L^2Cl{\cdot}2H_2O$]	45.0 (45.4)	3.1 (3.3)	11.9 (12.4)	6.7 (7.1)	12.7 (13)	7.6 (7.9)	16.3	3.1
C7	[Cu $L^2Cl{\cdot}2H_2O$]	44.4 (44.9)	2.9 (3.3)	8.9 (9.2)	6.7 (7.0)	13.5 (13.9)	7.5 (7.8)	21.5	1.73
C8	[Zn $L^2Cl{\cdot}2H_2O$]	44.4 (44.7)	3.0 (3.2)	11.9 (12.2)	6.8 (7.0)	14.0 (14.3)	7.3 (7.7)	14.4	Diamagnetic

recorded at room temperature on Varian E-4 X-band spectrometer using TCNE as g-marker. The Ostwald viscometer is used for hydrodynamic measurements.

Results and discussion

Chemistry

The analytical and physicochemical data of the complexes are summarized in Table 1. All complexes are soluble in organic solvents like DMF, DMSO and acetonitrile.

IR spectral studies

The IR spectra of the free ligands were compared with the spectra of the complexes. The IR spectral data and their assignments are depicted in the Table 2. The strong band at 1662 cm^{-1} in the ligand L^1H_3 is assigned to the amide carbonyl ν(C=O). The strong band in the region 1606 cm^{-1} in both the ligands was assigned to azomethine ν(C=N). The band at 1596 cm^{-1} in L^2H is assigned to the benzothiazole ring vibrations. Upon complexation azomethine ν(C=N) shows negative shift in (C1–C4) complexes, but in case of (C5–C8) complexes positive shift was observed. Collectively these observations signify the coordination of azomethine nitrogen (Guofa *et al*., 1990). Similarly benzothiazole ring vibrations {ν(C=N)} also show the negative shift in (C5–C8) complexes, which emphasize the involvement of benzothiazole ring nitrogen in the coordination. The negative shift of ν(C=O) group in all the complexes of L^1H_3 ligand suggests the coordination of amide carbonyl to the metal centre. The phenolic ν(OH) band is merged with stretching band of coordinated/lattice celled water molecules in the range 3350–3410 cm^{-1} in the complexes derived from L^1H_3. The complexes show a non-ligand band in the region 430–455 cm^{-1} ascribable to the ν(M–N) (Thomas *et al*., 1995).

Table 2 IR spectral data of the ligands and their complexes

Compounds	ν(C=N) Azomethine	ν(C=N) Benzothiazole	ν(C=O)	$\nu(H_2O)$
L^1H_3	1606	–	1662	3422
L^2H	1606	1596	–	3437
C1	1560	–	1637	3445
C2	1555	–	1634	3442
C3	1555	–	1610	3431
C4	1561	–	1610	3447
C5	1635	1549	–	3421
C6	1630	1555	–	3448
C7	1637	1545	–	3444
C8	1664	1568	–	3447

^1H NMR spectral studies

The ^1H NMR spectra of the ligands and their Zn(II) complexes were recorded in DMSO-d_6 solvent over the range of 0–16 ppm. Singlets in L^1H_3 and L^2H ligands at 8.7 and 8.3 ppm are assignable to the azomethine protons, which are shifted to down field region upon complexation with Zn(II) indicating the coordination of these functionalities (Chohan *et al*., 2004). In addition to this, a set of multiplet observed in the range 6.93–7.91 ppm is ascribed to the aromatic protons in all the compounds. The peak observed at 11.1 and 10.1 ppm in ligands is attributable to the –OH of quinoline molecule in L^1H_3 and L^2H, respectively. A sharp singlet at 12 ppm observed in the ligand L^1H_3 is due to –NH of amide carbonyl, which remains unaltered in the corresponding Zn(II) complex. The

absence of signal corresponding to quinoline –OH in (C4 and C8) complexes confirms the coordination of –OH group to the metal ion via deprotonation. The peak observed at 12.1 ppm in ligand L^1H_3 is assigned to the phenolic –OH which is retained in the C4 complex.

Molar conductivity measurements

Molar conductivities of the complexes were measured in DMSO solution with 10^{-3} M concentrations. All these complexes show molar conductance in the range 12–23 mho cm^2 mol^{-1} (Table 1). These low values of molar conductance of the complexes show that they are non-electrolytes (Geary, 1971).

Electronic spectral studies

The electronic spectra of the ligands and their complexes were recorded in DMSO solution. All the ligands exhibit similar features in UV-Visible region with the bands around 280 and 386 nm. The broad intense band around 280 nm in both the ligands can be assigned to intra ligand π–π^* transition. This band is almost unchanged in the spectra of all the complexes. The band at 385 nm with a shoulder on low energy side is due to n–π^* transition associated with the azomethine linkage. This band experiences red shift in all the complexes (Bhardwaj and Singh, 1994; Ainscough *et al*., 1997). The bands at around 420–460 nm are attributed to the ligand to metal charge transfer transitions.

Magnetic studies

The magnetic moment was recorded at room temperature and is shown in Table 1. The μ_{eff} values of (C1 and C5) complexes are found to be 4.43 and 4.45 BM suggesting octahedral geometry for both the C1 and C5 cobalt(II) complexes (Thakkar and Bootwala, 1995). The nickel(II) complexes (C2 and C6) have magnetic moment values of 2.95 and 3.1 BM which reveal the spin free octahedral configuration (Thakkar and Bootwala, 1995). The copper(II) complexes (C3 and C7) have μ_{eff} value less than the spin only value (1.69 and 1.73 BM) which accounts for metal-metal interaction. In support of other spectral data, magnetic moment values suggest square pyramidal geometry for C3 and octahedral geometry for C7.

EPR spectral studies

EPR studies of paramagnetic transition metal(II) complexes give information about the distribution of the unpaired electrons and hence about the nature of the bonding between the metal ion and its ligands.

The complex C3 exhibits a broad absorption signal with $g_{iso} = 2.02$, with no hyperfine splitting is observed in the spectrum of the complex.

The complex (C7) exhibits anisotropic signals with $g_{II} = 2.05$ and $g_{\perp} = 2.04$ values. From the observed trend, $g_{II} > g_{\perp}$, it is evident that the unpaired electron lies predominantly in the $d_{x^2-y^2}$ orbital with the possibility of some d_{z^2} character being mixed with it because of low symmetry (Kivelson and Neiman, 1961). The $g_{II} < 2.3$ indicates the larger percentage of covalency in metal to ligand bonds (Ray and Kuffman, 1989).

FAB mass studies

In the present investigation the FAB mass spectra of the C2, C3, and C7 complexes have been recorded and show a molecular ion peak at *m/z* 461, 906, and 459, respectively, which corresponds to the molecular weight of the respective complexes. Apart from this, the spectra show some other peaks correspond to the molecular cations of the complexes. The conclusion drawn from FAB mass spectra is that, the complex C3 is dimeric in nature where as the complexes C2 and C7 are monomeric.

Thermal analysis

The TG-DTA experiments were carried out to explore the thermal stability of the complexes. The thermal behaviors of all the metal complexes were studied in temperature range of 25–800°C. The TG-DTA studies of complexes C3 and C6 reveal that the decomposition proceeds in three steps. In the first stage weight loss at 98°C corresponds to the presence of the lattice cell water in both the complexes. The weight losses in the temperature range 110–200°C are due to the presence of the coordinated water in both the complexes. This is marked by endothermic peaks in DTA curves. A plateau was obtained after heating above 600°C, which corresponds to the formation of stable metal oxide.

Biochemistry

The ligands and their complexes C1–C8 were screened for antibacterial activity against *E. coli* and *Pseudomonas aeruginosa* and antifungal activity against *Aspergillus niger* and *Cladosporium*. The data are shown in Table 3. The compounds which show the promising antibacterial and antifungal activity were selected for minimum inhibitory concentration studies, which are determined by assaying at 250 μg concentrations along with standards at the same concentrations. Even at the MIC level the complexes C3, C4, and C7 were found to be more active against bacteria and fungi than the Schiff base

Table 3 Screening of compounds against bacteria and fungi

Compounds	*E. coli*		*Pseudomonas aeruginosa*		Compound name	*Aspergillus niger*		*Cladosporium*	
	Zone of inhibition in cm	% Inhibition	Zone of inhibition in cm	% Inhibition		Zone of inhibition in cm	% Inhibition	Zone of inhibition in cm	% Inhibition
Gentamycin	3.2	100	2.9	100	Flucanozole	1.2	100	0.9	100
L^1H_3	1.2	37.5	0.5	17.24	L^1H_3	0	0	0.2	22.2
C1	0.7	21.87	0.4	13.79	C1	0.2	16.6	0.1	11.1
C2	1.1	34.37	1.1	37.9	C2	0.4	33.3	0.1	11.1
C3	2.8	87.5	1.5	51.72	C3	0.6	66.6	0.4	44.4
C4	1.4	43.75	1.2	41.39	C4	1	83.3	0.6	66.6
L^2H	1.8	56.25	0.5	17.24	L^2H	0.1	8.3	0.5	55.5
C5	0.2	6.2	0.2	6.89	C5	0	0	0.2	22.2
C6	0.2	6.2	0	0	C6	0	0	0	0
C7	0.3	9.37	0.4	13.79	C7	0.7	58.3	1.1	122.2
C8	1.2	37.5	0.3	10.3	C8	0.6	50	0.4	44.4
DMF	0	0	0	0	DMF	0	0	0	0

ligands (Tables 4 and 5). This enhancement in the activity can be explained on the basis of chelation theory (Thimmaiah *et al*., 1985; Franklin and Snow, 1971). Such a chelation could enhance the lipophilic character of the central metal atom, which subsequently favors it permeation through the lipid layers of cell membrane (Jadon *et al*., 1996) and blocking the metal binding sites on enzymes of microorganism. The variation in the effectiveness of different compound against different organisms also depends on a nature of the metal ion, nature of the ligand, geometry of the complexes, and impermeability of the cell of the microbes or differences in ribosomes of microbial cells (Aliye *et al*., 2009; Sengupta *et al*., 1998; Kurtoglu *et al*., 2006).

Table 4 Antibacterial studies of compounds in MIC (250 μg) level

Compounds	*E. coli*		*Pseudomonas aeruginosa*	
	Zone of inhibition in cm	% Inhibition	Zone of inhibition in cm	% Inhibition
Gentamycin	3.2	100	2.9	100
L^1H_3	0.7	21.87	0.2	6.89
C3	2.1	65.62	1.1	37.93
C4	0.9	28.1	0.8	27.5
L^2H	0.6	18.75	–	–
DMF	0	0	0	0

Table 5 Antifungal studies of compounds in MIC (250 μg) level

Compounds	*Aspergillus niger*		*Cladosporium*	
	Zone of inhibition in cm	% Inhibition	Zone of inhibition in cm	% Inhibition
Flucanozole	1.2	100	0.9	100
C4	0.9	75	0.1	11.1
C7	0.3	25	0.9	100
DMF	0	0	0	0

Absorption studies

Electronic absorption spectroscopy is universally employed to determine the binding of complexes with DNA. The interaction of complexes with DNA causes electronic perturbations in the transition metal complexes at the maxima. The data obtained from this experiment shows a significant hypochromism with an insignificant blue shift at the maxima when increasing amounts of *E. coli-DNA* were added to the solution of complex. The extent of spectral change is related to the strength of binding of the complexes to *E. coli* DNA. These spectral characteristics suggest that, the complexes bound to *E. coli* DNA by an intercalative mode. Both the ligands have no effect on the absorption of DNA solution. The representative absorption spectrum of the nickel (C6) complex is given in Fig. 2. The intrinsic binding constant Kb obtained for C1–C8 complexes are given in the Table 6. By observing the intrinsic binding constant of all the complexes it has been suggested that the C6 and C7 complexes show more binding property than the remaining complexes.

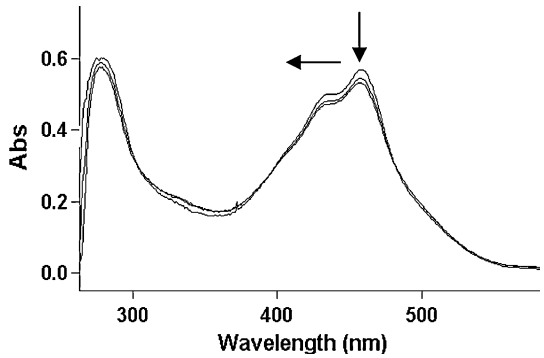

Fig. 2 Absorption spectrum of Nickel (C6) complex in Tris buffer upon addition of *E. coli*-DNA with complex

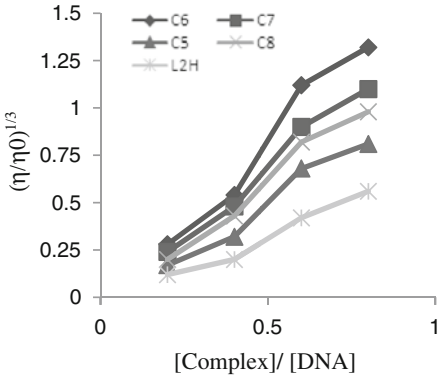

Fig. 3 Effect of increasing amounts of the ligand (L^2H) and its complexes (C5–C8) on the relative viscosities of *E. coli* DNA

Table 6 DNA binding constant of the complexes

Compounds abbreviations	Complexes	Binding constant Kb in M^{-1}
C1	$[Co\ L^1Cl{\cdot}2H_2O]{\cdot}H_2O$	1.08×10^3
C2	$[Ni\ L^1Cl{\cdot}2H_2O]{\cdot}H_2O$	1.63×10^3
C3	$[Cu\ L^1Cl]_2{\cdot}4H_2O$	1.53×10^3
C4	$[Zn\ L^1Cl{\cdot}2H_2O]{\cdot}H_2O$	1.31×10^3
C5	$[Co\ L^2Cl{\cdot}2H_2O]$	1.26×10^3
C6	$[Ni\ L^2Cl{\cdot}2H_2O]$	2.06×10^4
C7	$[Cu\ L^2Cl{\cdot}2H_2O]$	1.43×10^4
C8	$[Zn\ L^2Cl{\cdot}2H_2O]$	1.07×10^4

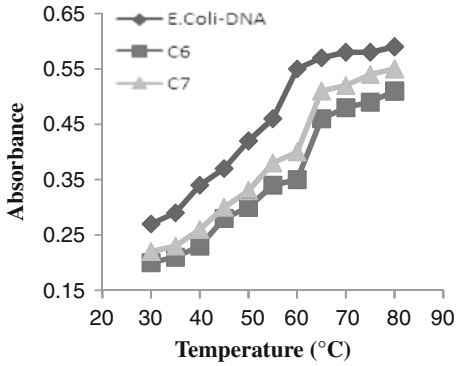

Fig. 4 Melting curves of *E. coli*-DNA in the absence and presence of complexes Nickel (C6) and Copper (C7)

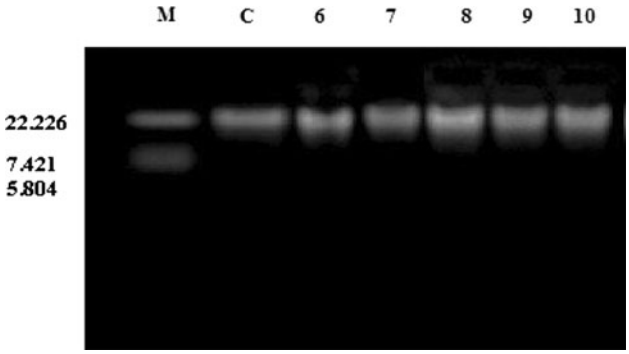

Fig. 5 Agarose gel showing the results of electrophoresis of *E. coli*-DNA with the Schiff base ligand L^2H and its complexes (C5–C8) [*M* standard molecular weight marker, *C- E. coli* control DNA of *E. coli*, *6* ligand (L^2H), *7* Cobalt (C5), *8* Nickel (C6), *9* Copper(C7), and *10* Zinc (C8)]

Viscosity measurement study

To further clarify the binding modes of the complexes with DNA, viscosity measurements were carried out. Spectroscopic experiments provide necessary data, but not sufficient clues to support a binding mode. Viscosity measurements that are sensitive to length change are regarded as the least ambiguous and the most critical tests of the binding model in solution in the absence of crystallographic structural data (Satyanarayana *et al*., 1992). The viscosity of DNA increases as the increase in the ratio of complexes to DNA indicates the intercalative mode of binding (Satyanarayana *et al*., 1992). The representative graph of the ligand L^2H and its complexes is shown in Fig. 3. The extent of intercalation observed is more in the nickel (C6) and copper (C7) complexes.

Thermal denaturation study

Thermal behaviors of DNA in the presence of complexes can give insight into their conformational changes when temperature is raised, and provide the information about the interaction strength of complexes with DNA (Kelly *et al*., 1985). The T_m of *E. coli* DNA in absence of the complexes is found to be 58 ± 1°C (Tselepi-Kalouli and Katsaros, 1989). (as shown in Fig. 4). On the bases of viscometric measurements the complexes C6 and C7 have chosen for the thermal denaturation experiment, because of their stronger binding capability with the *E. coli* DNA than any other complexes. However, with addition of nickel

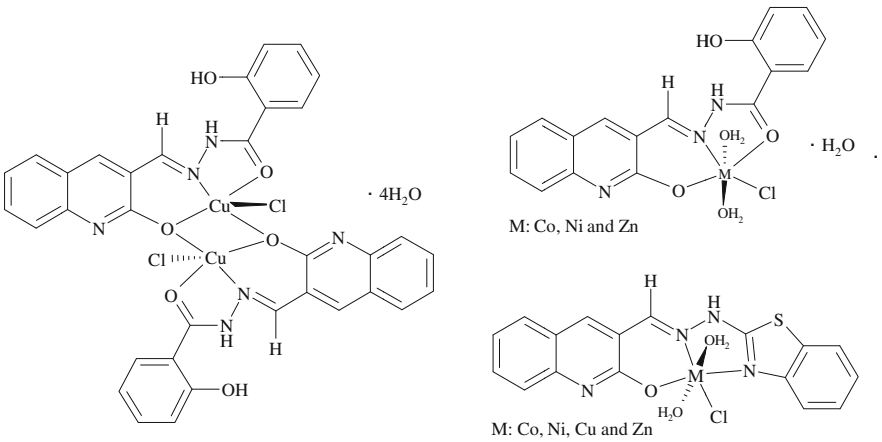

Fig. 6 The proposed structures of the complexes are shown below

(C6) and copper (C7) complexes, the T_m of the DNA increases dramatically to 65 ± 1°C. This is characteristic of an intercalative binding behavior of the complexes (López *et al*., 1996).

DNA cleavage studies using gel electrophoresis

The cleavage efficiency of the metal complexes compared to that of control is due to their efficient DNA binding ability. Both the ligands and complexes were allowed to interact with the *E. coli* DNA for cleavage study. In the present investigation, the nickel (C6) and copper (C7) complexes have shown increase in the intensity and tailing compared to remaining compounds which illustrates the higher binding ability of the said complexes with *E. coli* DNA (shown in a Fig. 5).

Conclusion

Based on the above results and discussion, it is concluded that the complexes have 1:1 metal to ligand stoichiometry; complex C3 is dimeric in nature where as remaining all are monomeric. Coordination behavior of Schiff base ligands is in tridentate manner which is evidenced by the elemental analysis and the spectral data, with NO_2 and N_2O donor sites. The geometry around the central metal ion in Co(II), Ni(II), Cu(II), and Zn(II) complexes was found to be an octahedral. But in case of C3 the geometry is square pyramidal.

The metal complexes have higher antimicrobial activity than the ligand, specially Cu(II) complexes have shown more activity even at the MIC level. In addition, the interaction of the ligands and their complexes with *E. coli* DNA was investigated by absorption, thermal denaturation, and viscosity measurements. These methods indicate that the complexes C6 and C7 bind to DNA, with higher affinity than the other ligand and complexes. The proposed structures of the complexes are given in a Fig. 6.

Acknowledgments The authors thanks the staff of department of chemistry and USIC, Karnatak University, Dharwad for providing research and spectral facilities. Recording of FAB mass spectra (CDRI Lucknow) and EPR spectra (IIT Bombay) is gratefully acknowledged. Further, the authors thank UGC for providing RFSMS and Karnatak University, Dharwad for providing research fellowships.

References

Ainscough EW, Brodie AM, Ranford JD, Waters JM (1997) Reaction of anionic oxygen donors with the antitumour copper(II)-pyridine-2-carbaldehyde thiosemicarbazone (HL) system and the crystal structure of $[\{Cu(HL)(H_2PO_4)\}_2][H_2PO_4]_2{\cdot}2H_3PO_4{\cdot}2H_2O$. J Chem Soc Dalton Trans 7:1251–1255

Aliye A, Nursen S, Naki, Hatice O (2009) Synthesis and biological activity of new cycloalkylthiophene-Schiff bases and their Cr(III) and Zn(II) complexes. Med Chem Res. doi: 10.1007/s00044-009-9214-8

Bhardwaj NC, Singh RV (1994) Sulphur-bonded thallous complexes of thiosemicarbazones. Indian Acad Sci (Chem Sci) 106:15–22

Chan S, Wong WT (1995) Synthesis, structure and DNA-binding studies on the 2-(3-chlorophenyl)imidazo[4, 5-f]1, 10-phenanthroline-bis(2, 2′-bipyridine)-ruthenium(II) complex. Coord Chem Rev 138:196–219

Chohan H, Humayun P, Rauf A, Khalid MK, Claudiu TS (2004) Isatin-derived antibacterial and antifungal compounds and their transition metal complexes. J Enzyme Inhib Med Chem 19: 417–423

Dang XJ, Nie MY, Tong J, Li HL (1998) Inclusion of the parent molecules of some drugs with β-cyclodextrin studied by electrochemical and spectrometric methods. J Electroanal Chem 448:61–67

Erkkila KE, Odom DT, Barton JK (1999) Recognition and reaction of metallo intercalators with DNA. Chem Rev 99:2777–2795

Franklin TJ, Snow GA (1971) Biochemistry of antimicrobial action, 2nd edn. Chapman and Hall, London

Freixas BJ, Span ES (1991) Preparation of 3-quinoline carboxylic acid derivatives as antibacterials. Chem Abstr 114:185302

Geary WJ (1971) The use of conductivity measurements in organic solvents for the characterisation of coordination compounds. Coord Chem Rev 7:81–122

Gracheva IN, Gridneva LI, Tochilkin AI, Gorkin VZ (1988) Hydrazides and sulfonyl hydrazides from the series of quinoline are human serum amine oxidase inhibitors. Khimiko Farmatsevticheskii Zhurnal 22:1336–1339

Guofa L, Chowngwu N, Bin L, Kunyuan M (1990) Complexes of lanthanide nitrates with a Schiff base derived from o-vanilline and p-toluidine. Polyhedron 9:2019–2022

Hagen H, Dupuis J, Wuerzer B, Germanoffen DE (1988) 8-quinoline carboxylic acid derivatives, procedure for their preparation and their use as herbicides. Chem Abstr 109:149370

Jadon SCS, Singh D, Singh RV (1996) Ruthenium (III) and rhodium (I) chelates of azomethines derived from 1-(2-naphthenyl)ethanone. Indian J Chem 35:1107–1110

Kelly JM, Tossi AB, McConnell DJ, OhUigin C (1985) A study of the interactions of some polypyridyl ruthenium (II) complexes with DNA using fluorescence spectroscopy, topoisomerisation and thermal denaturation. Nucleic Acids Res 13:6017–6034

Kivelson D, Neiman R (1961) ESR studies on the bonding of copper complexes. J Chem Phys 35:149–155

Kurtoglu M, Dagdelen MM, Toroglu S (2006) Synthesis and biological activity of novel (E, E)-vic-dioximes. Trans Met Chem 31:382–388

Liang F, Wang P, Zhou X, Li T, Li ZY, Lin HK, Gao DZ, Zheng CY, Wu CT (2004) Copper complex of hydroxyl-substituted triaza-macrocyclic ligand and its antitumor activity. Bioorg Med Chem Lett 14:1901–1917

López RB, Loeb BL, Boussie T, Meyer TJ (1996) Synthesis of a new phenanthroline derived ligand with acceptor properties. Tetrahedron Lett 37:5437–5440

Meth-Cohn O, Narine B (1978) A versatile new synthesis of quinolines, thienopyridines and related fused pyridines. Tetrahedron Lett 23:2045–2048

Pratviel G, Bernadou J, Meunier B (1998) Oxidation of guanine bases mediated by a manganese-porphyrin-oligonucleotide conjugate onto a G-rich DNA target: 8-oxo-7, 8-dihydroguanine is not the major lesion. Adv Inorg Chem 45:251

Rao S, Mishra DD, Mourya RV, Nageswara N (1997) Oxovanadium binuclear (IV) Schiff base complexes derived from aroyl hydrazones having subnormal magnetic moment. Polyhedron 16:1825–1829

Ray RK, Kauffman GB (1989) Chromatographic studies of metal complexes. Part IV. Thin layer chromatographic separation of cis from trans isomers of cobalt (III) mixed ligand complexes. Inorg Chim Acta 162:45–48

Revankar VK, Arali VH, Mahale VB (1990) Synthesis, characterization and biological studies of 3-acetylcoumarin hydrazones with cobalt(II), nickel(II) and copper(II). Indian J Chem 29:889–894

Ryoichi A, Junichi O, Japan Kokai Tokyo Koho JP (1991) Preparation of quinolones as bioavailability improved oral bactericides. Chem Abstr 114:185301n

Sarma RH (1980) Nucleic acid geometry and dynamics. Pergamon Press, New York, pp 83–108

Satyanarayana S, Dabrowiak JC, Chaires JB (1992) Neither D- nor L-tris (phenanthroline) ruthenium (II) binds to DNA by classical intercalation. Biochemistry 31:9319–9324

Seeley HW (1991) Microbes in action. A laboratory manual of microbiology, 4th edn. Cornell University, Ithaca

Sengupta SK, Pandey OP, Srivastava BK, Sharma VK (1998) Synthesis, structural and biochemical aspects of titanocene and zirconocene chelates of acetylferrocenyl thiosemicarbazones. Trans Met Chem 23:349–353

Thakkar NV, Bootwala SZ (1995) Synthesis and characterization of binuclear metal complexes derived from some isonitrosoacetophenones and benzidine. Indian J Chem 34:370–374

Thimmaiah KN, Lloyd WD, Chandrappa GT (1985) Stereochemistry and fungitoxicity of complexes of p-anisaldehyde thiosemicarbazone with Mn(II), Fe(II), Co(II) and Ni(II). Inorg Chim Acta 106:81–83

Thomas M, Nair MKM, Radhakrishnan RK (1995) Rare earth iodide complexes of 4-(2′, 4′-dihydroxyphenylazo) antipyrine. Synth React Inorg Met Org Chem 25:471

Tselepi-Kalouli E, Katsaros N (1989) The interaction of $[Ru(NH3)5Cl]^{2+}$ and $[Ru(NH3)6]^{3+}$ ions with DNA. J Inorg Biochem 37:271–282

Vogel AI (1968) A text book of practical organic chemistry. ELBS, Longmans Green, London

West DX, Liberta AE, Padhye SB, Chikate RC, Sonawane PB, Kumbhar AS, Yerande RG (1993) Thiosemicarbazone complexes of copper(II): structural and biological studies. Coord Chem Rev 123:49–71